JOURNAL OF MATERIALS SCIENCE **34** (1999) 3155–3159

Brittle-to-ductile transition temperature and its strain rate sensitivity in a two-phase titanium aluminide with near lamellar microstructure

YU WANG, DONGLIANG LIN (T. L. LIN)
Department of Materials Science, Shanghai Jiaotong University, Open Laboratory of Education Ministry for High-Temperature Materials and Tests, Shanghai, 200030, People's Republic of China

CHI C. LAW
Materials & Mechanics Engineering, United Technologies—Pratt & Whitney, East Hartford, Connecticut, 06108, USA
E-mail: dllin@mail.sjtu.edu.cn

The temperature dependence of tensile properties of a two-phase titanium aluminide with nearly lamellar microstructure has been investigated and brittle-to-ductile transition (BDT) temperatures (T_{BDS}) have been determined under different strain rates from 10^{-5} to 10^{-1} s^{-1}. It is found that T_{BD} rises with the increase of strain rate. From the positive strain rate sensitivity of T_{BD}, the apparent activation energy of BDT is determined to be 324 kJ/mol by means of Zener-Hollomon factor. The determined activation energy approximates to the activation energies of self-diffusion of Ti atoms, and inter-diffusion of Ti and Al atoms in TiAl phase. The approximation, fractography analysis and theoretical calculation using the Nabarro Model add up to the speculation that the BDT of the alloy is controlled by dislocation climbing.

1. Introduction

γ-TiAl/α_2-Ti_3Al two-phase intermetallics (hereafter referred to as the TiAl alloy) have recently received increasing attention because of their potential as structural materials for high temperature applications. TiAl alloy is brittle at room temperature but becomes ductile at high temperature, manifesting brittle-to-ductile transition (BDT) in the intervening temperature range. It has been found that the brittle-to-ductile transition temperature (T_{BD}) of the alloy, which usually ranges from 600 to 820 °C, depends on chemical composition and microstructure of the alloy and that alloys with duplex (DP) microstructure have lower T_{BD} than those with fully lamellar (FL) or nearly lamellar (NL) microstructure [1, 2]. Moreover, T_{BD} was found qualitatively to go up with the strain rate in TiAl alloy with near gamma or DP microstructure by Lipsitts *et al*. [3], Seetharaman *et al*. [4] and Kumpfert *et al*. [5]. Nevertheless, none of Refs. [2–5], which addresses BDT in TiAl alloys, gives a quantitative criteria for T_{BD} evaluation. The relationship between T_{BD} and the strain rate has yet to be investigated quantitatively, especially in the alloy with FL or NL microstructure.

In this paper a two-phase titanium aluminide with NL microstructure is chosen to study the strain rate sensitivity of T_{BD}. The controlling mechanism of BDT is speculated accordingly.

2. Experimental

The chemical composition of the chosen alloy is Ti-47at %Al-2at %Mn-2at %Nb. The alloy was produced by vacuum melting technique, and then, was thermally mechanically processed into plates with a thickness of about 6 mm and heat treated to have NL microstructure at room temperature. Initial microstructure, the microstructure before deformation, was etched by a mixture of 2.5% volume of HF, 2.5% volume of HNO_3 and 95% volume of H_2O, and observed using a Neophot-II optical microscope.

Plate specimens with a gauge section of $15 \times 3.5 \times 1.8$ mm were used. The specimens were cut from the 6 mm-thick plates using an electro-discharging machine, polished by emery paper first and electropolished finally to eliminate their surface defects and damage. The polishing solution was a mixture of perchloric acid, *n*-butanol and methanol, whose volume ratio was 6:35:60, and the temperature and voltage were maintained at 213–223 K and 50 V, respectively.

Tensile tests were conducted on a Shimadzu AG-100kNA material testing machine. The initial strain rate, which is the ratio of constant velocity of the crosshead to the gauge length, 15 mm, was chosen as 10^{-5}, 10^{-4}, 10^{-3}, 10^{-2} and $10^{-1}s^{-1}$, respectively. The testing temperature was chosen as 285, 398, 523, 598, 673, 773, 873, 973, 1073, 1173, 1273 and 1373 K. For testing

temperature above 1073 K, the samples were covered with oxidation-proof coating.

The fracture morphology was analyzed by a S520-type scanning electron microscope (SEM), operating at an accelerating voltage of 20 kV.

3. Result

3.1. Initial microstructure

The initial microstructure of the alloy is shown in Fig. 1, which proves that the alloy possessed NL microstructure before tensile testing. The average size of lamellar colonies is about 0.5 mm.

3.2. The effect of temperature and strain rate on tensile properties

Fig. 2 shows the temperature dependence of yield strength ($\sigma_{0.2}$) and elongation (δ) under different strain rates. As can be seen in Fig. 2, under the strain rate of $10^{-5}s^{-1}$, the yield strength starts to decrease sharply while the elongation starts to increase abruptly when the temperature rises to 973 K. If the temperature at which the elongation reaches 7.5% is defined as T_{BD}, the T_{BD} of the alloy is determined to be 1023 K under the strain rate of $10^{-5}s^{-1}$. The T_{BD}s under other strain rates are determined in the same way, and the results are tabulated in Table I, which shows that T_{BD} is sensitive to the strain rate, going up with the increase of the latter.

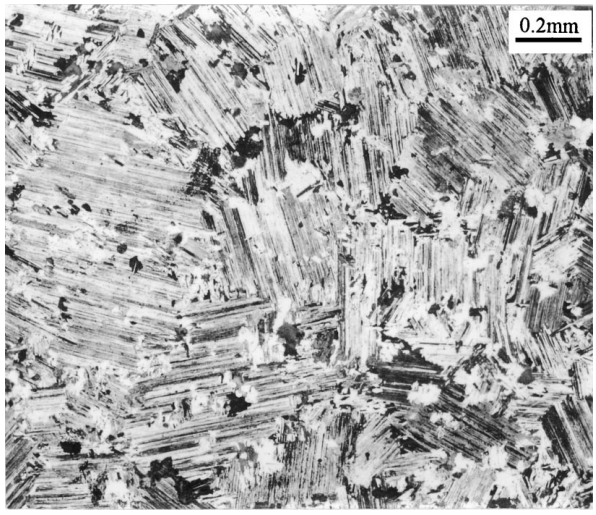

Figure 1 Initial microstructure.

TABLE I T_{BD} of the investigated alloy at different strain rates

Strain rate (s^{-1})	10^{-5}	10^{-4}	10^{-3}	10^{-2}	10^{-1}
T_{BD} (K)	1023	1098	1173	1273	>1373

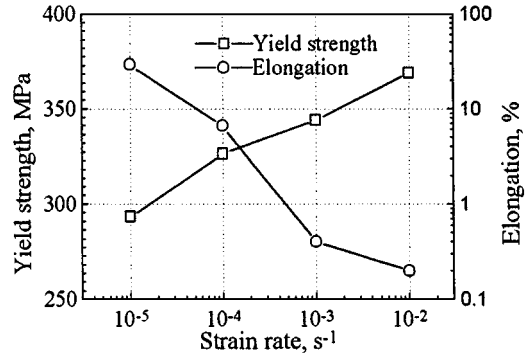

Figure 3 Variation of yield strength and elongation with the strain rate at 1073 K.

The strain rate dependence of $\sigma_{0.2}$ and δ at 1073 K is shown in Fig. 3. As the strain rate ascends, $\sigma_{0.2}$ rises while δ drops, similar to the circumstances in the case of lowering the temperature under a constant strain rate. In other words, raising the strain rate produces an equivalent effect on tensile properties to that of lowering the temperature.

3.3. Fractography

Fig. 4 are micrographs from samples fractured under the strain rate of $10^{-4}s^{-1}$. Transgranular cleavage, including translamellar cracking and delamination, appears to be the predominant mode of failure below T_{BD} (Fig. 4a) while dimple fracture plays the main role above T_{BD} (Fig. 4b).

Fig. 5 shows the fracture morphology of samples deformed at 1073 K under two different strain rates. Under the strain rate of $10^{-5}s^{-1}$, with the corresponding T_{BD} (1023 K) lower than the testing temperature, the fracture mode is dimple fracture while under the strain rate of $10^{-1}s^{-1}$, with the corresponding T_{BD} higher than the testing temperature, the fracture mode is mainly transgranular cleavage (Fig. 5b).

As can be seen from Figs 4 and 5, BDT seems to coincide with the emergence of numerous dimples on the fracture surface. Furthermore, from the similarity between Fig. 4a and Fig. 5b, Fig. 4b and Fig. 5a, increasing

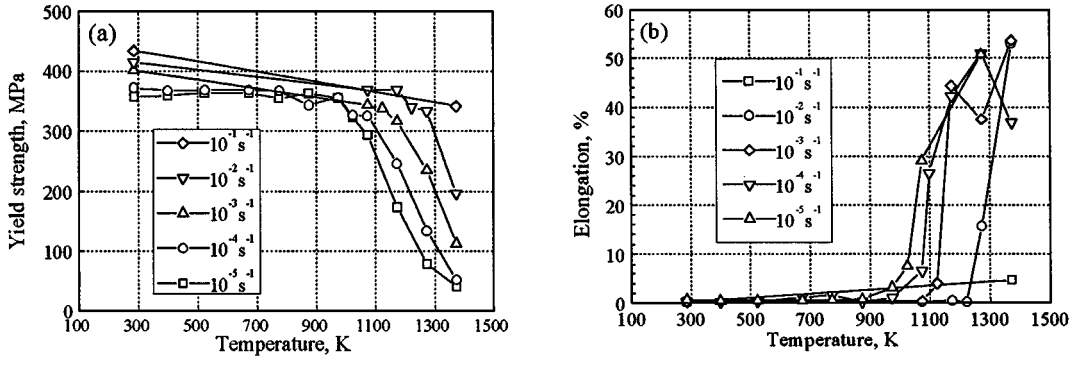

Figure 2 Temperature dependence of (a) $\sigma_{0.2}$ and (b) elongation under different strain rates.

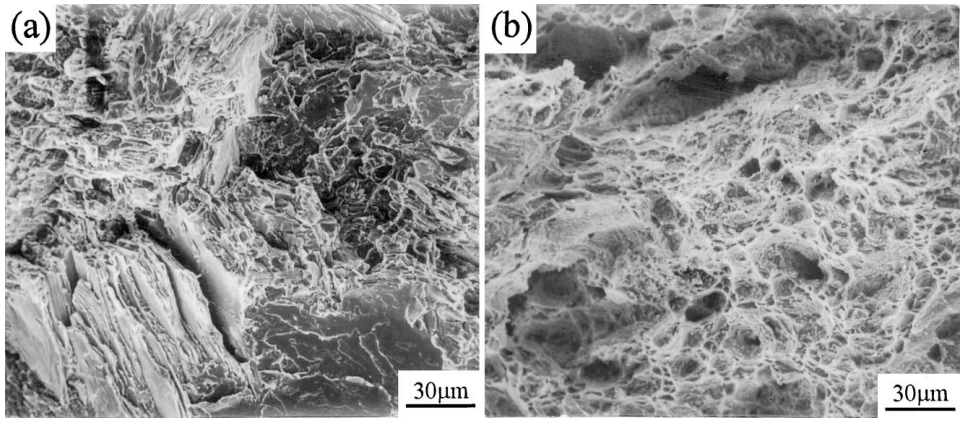

Figure 4 Fractographs at (a) 1073 K and (b) 1173 K under the strain rate of $10^{-4}s^{-1}$.

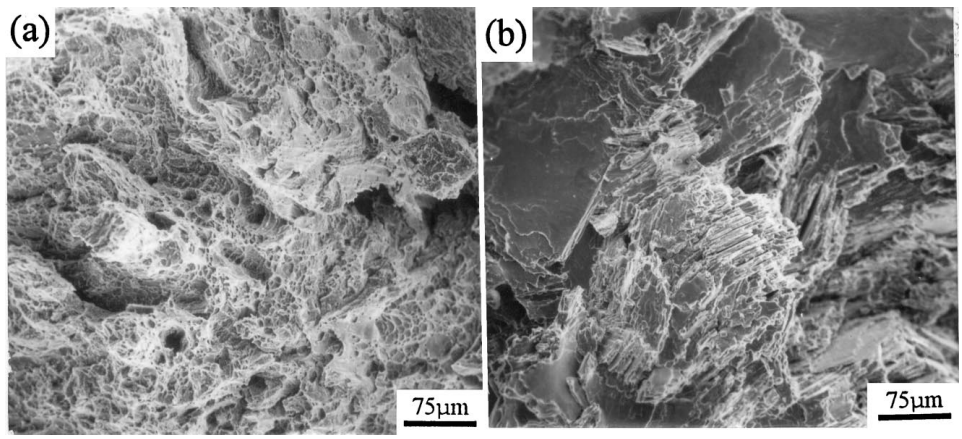

Figure 5 Fractographs under the strain rates of (a) $10^{-5}s^{-1}$ and (b) $10^{-1}s^{-1}$ at 1073 K.

strain rate and lowering temperature are found to produce equivalent effects on the fracture mode.

4. Discussion

4.1. The change in fracture mode and deformation mechanism above and below T_{BD}

Although it seems arbitrary to define T_{BD} as the temperature corresponding to 7.5% elongation in this paper, the definition is justified by the transition in fracture mode from transgranular cleavage below T_{BD} to dimple fracture above T_{BD}. Huang *et al*. has estimated T_{BD} in Ti-48Al alloy around 550 °C, but the tensile ductility of the Ti-48Al alloy they investigated is no more than 2.4% at 550 °C and rises to only 5% at 600 °C (see Fig. 9 in Ref. [2]). As the tensile ductility does not see a rapid increase around 550 °C, it is not persuasive to take 550 °C as T_{BD}.

The transition in fracture feature also suggests a change in the mechanism of deformation and fracture in the course of BDT. The equalivent effects lowering temperature and raising the strain rate produce on tensile properties and fractograph indicate that BDT is a thermally activated course. The suppression of dimple fracture by raising the strain rate to a level high enough further indicates that the deformation controlled by dimple-producing mechanism is low. Dimples, which form at high temperatures, may result from dislocation climbing.

4.2. The apparent activation energy of BDT

It is generally accepted that both temperature and strain rate affect mechanical properties. Zener and Holloman [6] reduced the effect of temperature and strain rate on mechanical properties to that of a factor, so-called Zener-Holloman factor, expressed by:

$$Z = \dot{\varepsilon} \exp(Q/RT) \tag{1}$$

where Q is apparent activation energy and R is ideal gas constant. According to Zener and Holloman, as long as the values of Z are equal with each other, the corresponding mechanical properties are also identical no matter what the combination of temperature and strain rate is [6].

Supposing that the Z value at T_{BD} is a constant, Equation 1 can be converted into

$$\ln \dot{\varepsilon} = \ln Z - Q/RT_{BD} \tag{2}$$

which means that $\ln \dot{\varepsilon}$ has linear relationship with $1/T_{BD}$. The linear slope is $-Q/R$. Using the data in Table I, $\ln \dot{\varepsilon}$ is plotted against $1/T_{BD}$ in Fig. 6, which shows that the natural logarithm value of the strain rate indeed has linear relationship with $1/T_{BD}$. From the slope of the regressive line in Fig. 6, the apparent activation energy of BDT is determined to be 324 kJ/mol. The value approximates to 291 kJ/mol [7], the self-diffusion activation energy of Ti atom in single-phase

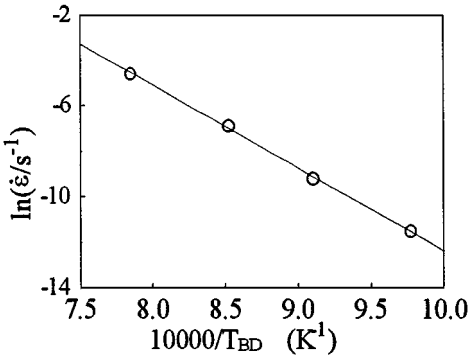

Figure 6 $\ln \dot{\varepsilon}$ plotted against $1/T_{\mathrm{BD}}$.

TiAl alloy, and 295 kJ/mol [8], the inter-diffusion activation energy of Ti and Al atoms in TiAl phase. The approximation points to that the BDT course of the alloy is controlled by an atomic diffusion process.

4.3. The contribution of dislocation climbing to deformation rate

Generally speaking, deformation is undertaken by dislocation motion. Although twinning is often argued to play a role in the deformation of TiAl alloy [2, 3], it results from the motion of $1/6 < 112$ partial dislocation. From the viewpoint of dislocation motion, diffusion controlled deformation at high temperature can only be proceeded by dislocation climbing. According to the model of Nabarro [9], which is based on the theory of steady-state diffusion creep, the strain rate produced by dislocation climb is given by

$$\dot{\varepsilon} = \frac{Dbp^3}{\pi kTG^2} \Big/ \ln\left(\frac{4G}{\pi p}\right) \tag{3}$$

TABLE II Value or expressions of the parameters in Equation 3 used to estimate the strain rates which may be provided by dislocation climbing

Parameters	Value or expressions
D (m^2s^{-1})	$1.53 \times 10^{-4} \exp(-291000/RT)$ [7]– $2.80 \times 10^{-4} \exp(-295000/RT)$ [8]
b (m)	2.83×10^{-10} [10]
G (GPa)	$72.24 - 0.0141T$ [11]

where D, G and b are self-diffusion coefficient, shear modulus, and the magnitude of Burgers vector of the climbing dislocations, respectively; p is the flow stress externally applied; and k is Boltzmann constant.

Although the investigated alloy contains a minor phase of α_2-Ti_3Al, the small fraction of α_2 phase disqualifies the minor phase from controlling the plastic deformation rate of the whole alloy. As a good approximation, the deformation rate of the major γ phase is taken as that for the whole alloy. In order to calculate the $\dot{\varepsilon}$ in Equation 3 at 1073 K at three representative points: the yield point (yp), the maxim load point (max) and the necking point or fracture point when necking doesn't occur (n/b), the value of the parameters in Equation 3 are taken as those of γ phase (listed in Table II). The inter-diffusion coefficient of Ti and Al atoms measured by Sprengel *et al*. [8] and the self-diffusion coefficient of Ti atom measured by Kroll *et al*. [7] are taken as upper and lower limit of D, respectively, and the Burgers vector magnitude of $1/2 < 110]$ dislocations, which are found most popular at high temperature [10], is chosen as b. The calculation result, as well as the experimentally applied strain rates for comparison, are listed in Table III.

The data in Table III show that at the lowest initial strain rate, $10^{-5}s^{-1}$, the strain rates produced by dislocation climbing approach or exceed the externally applied rates; when the applied initial strain rate rises to $10^{-4}s^{-1}$, the strain rates produced by climbing are less than that externally applied by 1.5–7.5 times; when the applied initial strain rate rises further to 10^{-3} and $10^{-2}s^{-1}$, the strain rates produced by climbing lags behind the externally imposed rates by 1–2 orders of magnitude. The comparison between applied and calculated rates shows that under the initial strain rate of $10^{-5}s^{-1}$ climbing is fast enough to undertake the applied strain rate while under the initial strain rates around $10^{-4}s^{-1}$, climbing start to not be able to keep up with the applied strain rate and gliding and twinning have to be considered to be mainly responsible for plastic deformation. At 1073 K, the alloy manifests BDT around the strain rate of $10^{-4}s^{-1}$. Whether the alloy is brittle or ductile coincides with whether dislocation climbing can keep up with the externally imposed strain rate or not, which is also found by Kad and Fraser [10] in compression of single-phase γ-TiAl alloy.

The change in fracture mode below and above T_{BD}, the approximation of activation energy of BDT to those of atomic diffusion in TiAl phase, and the concurrence of dislocation climbing and good ductility lead to the

TABLE III Comparison of the estimated strain rates, using Equation 8, provided by dislocation climbing with the externally applied strain rates at 1073 K

Initial strain rate (s^{-1})	D ($\times 10^{-18}$ m^2s^{-1})	G (GPa)	True stress measured p (MPa)			Estimated strain rate ($\times 10^{-5}s^{-1}$)			Externally applied true strain rate ($\times 10^{-5}s^{-1}$)		
			yp	max	n/b	yp	max	n/b	yp	max	n/b
10^{-5}			294	364	258	0.829–0.972	1.64–1.92	0.548–0.643	0.998	0.958	0.803
10^{-4}	1.04–1.22		327	449	449	1.17–1.37	3.21–3.76	3.21–3.76	9.98	9.44	9.38
10^{-3}		59.11	345	375	375	1.38–1.61	1.80–2.11	1.80–2.11	99.8	99.6	99.6
10^{-2}			370	370	370	1.72–2.02	1.72–2.02	1.72–2.02	998	998	998

speculation that the BDT in the investigated TiAl alloy is initiated by dislocation climbing. The speculation has been confirmed by Appel *et al*. [12], who deduced the same conclusion from their thermal activation analysis and transmitting electron microscopy observation on several TiAl alloys.

5. Conclusion

(1) The T_{BD} of TiAl alloy with nearly lamellar microstructure depends sensitively on the strain rate. It increases from 1023 K to above 1373 K as the strain rate increases from $10^{-5}s^{-1}$ to $10^{-1}s^{-1}$.

(2) The fracture mode of the alloy is affected by temperature and strain rate. Transgranular cleavage (including translamellar cleavage and delamination) dominates below T_{BD} while dimple fracture plays the main role above T_{BD}.

(3) The brittle-to-ductile transition of the alloy is a thermally activated process and its apparent activation energy is 324 kJ/mol, approximate to the activation energies of self-diffusion of Ti atoms, and inter-diffusion of Ti and Al atoms in TiAl phase.

(4) BDT course is speculated to be initiated by dislocation climbing.

Acknowledgement

This work was supported by United-Technologies—Pratt & Whitney, USA, and the National Natural Science Foundation of China.

References

1. Y. W. KIM, *JOM* **46** (1994) 30–40.
2. S. C. HUANG and E. L. HALL, *Metall. Trans. A* **22** (1991) 427–439.
3. H. A. LIPSITT, D. SCHECHTMAN and R. E. SCHAFRIK, *ibid.* 1975; 6:1991.
4. V. SEETHARAMAN, S. L. SEMIATIN, C. M. LOMBARD and N. D. FREY, *Mater. Res. Soc. Symp. Proc.* **288** (1993) 513–518.
5. J. KUMPFERT, Y-W. KIM and D. M. DIMIDUK, *Mater. Sci. Eng. A* **192/193** (1995) 465–473.
6. C. ZENER and J. HOLLOMON, *J. Appl. Phys.* **15** (1994) 22–32.
7. S. KROLL, H. MEHRER *et al., Z. Mettallkd.* **83** (1992) 591–595.
8. W. SPRENGEL, N. OIKAWA and H. NAKAJIMA, *Intermetallics* **4** (1996) 185–189.
9. F. R. N. NABARRO, *Phil. Mag.* **16** (1967) 231–240.
10. B. K. KAD and H. L. FRASER, *ibid.* **69** (1994) 689–699.
11. R. E. SCHAFRIK, *Metall. Trans. A* **8** (1977) 1003–1006.
12. F. APPEL, U. LORENZ, M. OEHRING, U. SPARKA and R. WANGNER, *Mater. Sci. Eng. A* **233** (1997) 1.

Received 27 July 1998
and accepted 22 January 1999